One- and Two-Dimensional Shadowing Functions for any Height and Slope Stationary Uncorrelated Surface in the Monostatic and Bistatic Configurations

Christophe Bourlier, Gérard Berginc, and Joseph Saillard

***Abstract*—The approaches developed by Wagner [1] and Smith [2], [3] for computing the shadowing properties from a one-dimensional randomly stationary surface are investigated for an arbitrary surface uncorrelated height and slope probability density function (pdf) and extended to a two-dimensional surface in the monostatic and bistatic configurations. Bourlier *et al.* [5] have expressed, from Brown's work [4], the Smith and Wagner average shadowing functions, for a one-dimensional surface, whatever the assumed uncorrelated slope and height pdf. They are then completely defined from both integrations over the surface slope pdf. The shadowing function is performed for Gaussian, Laplacian, and exponential slope probability density functions. With the method presented in [6], the one-dimensional monostatic shadowing function is also compared with the exact solution. It is obtained by generating the slope-height surfaces. The Gaussian and Laplacian slope pdfs are treated with a Gaussian surface height. The analytical results are extended to a one-dimensional bistatic configuration, and the case of a two-dimensional surface is investigated with a Gaussian and Laplacian surface slope pdfs. The last point is very relevant, because the classical shadowing functions of Smith and Wagner are assumed to be one-dimensional or isotropic.**

***Index Terms*—Electromagnetic scattering by rough surfaces, shadowing function.**

I. Introduction

THE shadowing function of random surfaces is originally introduced as a correction to the unshadowed scattering coefficient performed from analytical formulations as the Kirchhoff approach. With the geometric optics approximation derived from the Kirchhoff integral, [7] shows how the shadow can be introduced in the scattering coefficient from the use of the average shadowing function over the surface slopes and heights. Theoretically, the scattered field Kirchhoff integral and the statistical shadowing function (the average over the slopes and the heights is not performed) from random surfaces depend on the surface slopes and heights. This means that the statistical shadowing function should be included in scattered field, and the shadowed scatttering coefficient is obtained from averaging the shadowed scattered field multiplied by its conjugate. Bourlier *et al.* exposed this problem in [8] and [9] with the Kirchhoff formulation.

Manuscript received May 29, 2001.

C. Bourlier and J. Saillard are with IRCCyN: UMR no. 6597 CNRS, Division SETRA, Ecole Polytechnique de l'Université de Nantes, IRESTE, 44306 Nantes Cedex 3, France (e-mail: cbourlie@ireste.fr).

G. Berginc is with DS/DFO, Thomson-CSF Optronique, 78283 Guyancourt Cedex, France.

Publisher Item Identifier S 0018-926X(02)02622-4.

The scattering analytical theories and the shadowing function are developed with a slope and height joint Gaussian process. Gaussian process is probably adequate for the ocean, but for other surfaces such as sea ice, the density function of the surface roughness is not Gaussian [10]. Therefore, it is necessary to extend the shadowing theory for any density function in order to study its effect; such is the purpose of this paper.

References [11] and [12] proved that the shadowing function is rigorously defined by Rice's infinite series of integrals. In [6], Bourlier *et al.* observe that the approach proposed by Wagner retains only the first term of these series, whereas the Smith formulation uses the Wagner model by introducing a normalization function. The average shadowing function with the Ricciardi–Sato solution has been calculated with a Gaussian uncorrelated process [6], and since the correlation between the surface slopes and heights is ignored, the solution has not physical meaning at grazing incidence angles. Therefore, the Smith and Wagner approaches are used to study the shadowing effect of a random surface, because the Ricciardi–Sato formulation is not tractable with correlation.

Classically, the surface is assumed to be one-dimensional with a stationary Gaussian probability density function (pdf), and the correlation between the slopes and the heights is omitted. In [5] and [6], the last assumption has been investigated for any one-dimensional surface-height autocorrelation function, and it is proved that the discrepancy between the correlated and uncorrelated results is small. Consequently, in this paper, the correlation is not investigated, which allows a simpler formulation of the shadowing function. However, the shadowing function is determined for any surface slope and height pdf. From Brown's work [4] with a one-dimensional surface, Bourlier *et al.* [5] have expressed the Smith and Wagner monostatic shadowing functions, averaged over the surface slopes and heights, whatever the slope and height pdf assumed to be uncorrelated. These average monostatic shadowing functions depend then on two integrations over the surface slope pdf and independent of the surface height pdf.

In Section II, the results are applied to Gaussian, Laplacian, and exponential slope probability density functions. Moreover, for a Gaussian surface height autocorrelation function of Gaussian surface height pdf, the shadowing functions are compared with the exact solution [6], [13]. The exact solution is calculated numerically by generating the height and slope surfaces. Since it is difficult to simulate a surface of exponential pdf, the Gaussian and Laplacian slope pdfs are only treated in this paper. Note that the relationship between Laplacian

and Gaussian samples has to be determined. In Section III, the monostatic case is extended to the bistatic configuration. From the approach developed by [5] in Gaussian case, the last section presents the two-dimensional shadowing function with Gaussian and Laplacian slope distributions.

II. One-Dimensional Surface for a Monostatic Configuration

References [11] and [12] give the rigorous expression of the statistical shadowing function equal to Rice's infinite series of integrals. For an uncorrelated Gaussian process, these series can be computed analytically, but as shown [6], the model does not have physical meaning at grazing incidence angles. Moreover, when the correlation is introduced, the problem becomes very complicated and is not tractable analytically [14]. Therefore, the Wagner approach [1], which keeps only the first term of Rice's series, and the Smith [2], [3] formulation, which uses Wagner's formulation with the introduction of the normalized function, are then studied for estimating the shadowing effect. Comparing these models with the exact solution, Bourlier *et al.* [5], [6] show that with a correlated Gaussian process and Gaussian and Lorentzian surface height autocorrelation functions, there is good agreement between the results.

The exact solution is computed from generating numerically the height and slope surfaces and using the algorithm of Brokelman–Hagfors [13] summarized in [6, Fig. 4]. Moreover, since with the same statistic properties as previously the deviation between the results obtained with and without correlation is small, in this paper the correlation between the surface slopes and heights is not investigated. This allows a simpler statistical shadowing function and implies that the shadowing effect is independent of the surface autocorrelation function.

This section presents the one-dimensional shadowing function for a monostatic configuration obtained from the Wagner and Smith analysis without correlation. With the aim to estimate the accuracy of their formulations, the exact solution is computed from generating the height and slope surfaces. Gaussian, Laplacian, and exponential slope probability density functions are studied in the determination of the analytical shadowing function. The exact solution is examined for Gaussian and Laplacian slope distributions with a surface Gaussian height pdf of Gaussian surface height autocorrelation function.

A. Wagner and Smith Formulations

For an infinite observation length, the statistical shadowing function $S(\theta, F)$ is equal to the probability that the point $F(\xi_0, \gamma_0)$ on a random rough surface, of given height ξ_0 above the mean plane and with local slope $\gamma_0 = \partial z/\partial y$, is illuminated as the surface is crossed by an incident beam from incidence angle θ (Fig. 1)

$$S(\theta, F) = \Upsilon(\mu - \gamma_0) \exp\left[-\int_0^\infty g(\theta|F; l)\, dl\right] \tag{1}$$

with

$$\Upsilon(\mu - \gamma_0) = \begin{cases} 0, & \text{if } \gamma_0 \geq \mu \\ 1, & \text{if } \gamma_0 < \mu \end{cases} \tag{1a}$$

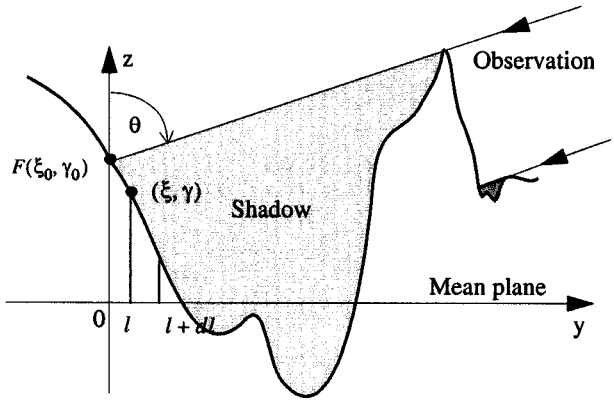

Fig. 1. Illustration of the monostatic shadowing function.

where $g(\theta|F; l)\, dl$ is the conditional probability that the ray intersects the surface in the interval $[l; l + dl]$ and knowing that the ray does not cross the surface in the interval $[0; l]$. Υ is the Heaviside function. In the Wagner (index W) and Smith (index S) approaches, $g(\theta|F; l)\, dl$ is defined as follows:

$$\begin{cases} g_W(\theta|F; l) = \displaystyle\int_\mu^\infty (\gamma - \mu) \times p(\xi, \gamma|\xi_0, \gamma_0)\, d\gamma \\ g_S(\theta|F; l) = \dfrac{g_W(\theta|F; l)}{\displaystyle\int_{-\infty}^{\infty} \int_{-\infty}^{\xi_0 + \mu l} p(\xi, \gamma|\xi_0, \gamma_0)\, d\xi\, d\gamma} \end{cases} \tag{2}$$

where $\xi = \xi_0 + \mu l$ and $p(\xi, \gamma|\xi_0, \gamma_0)$ is the surface slope $\{\gamma_0, \gamma\}$ and height $\{\xi_0, \xi\}$ conditional joint probability density. $\mu = \cot\theta$ is the slope of the incident ray. We can notice that Smith introduces a normalization function in the denominator. The exact formulation of $g(\theta|F; l)\, dl$ is expressed as an integral infinite series of Rice (for more details, see [11], [12], and [6]).

The uncorrelated surface pdf states that

$$p(\xi, \gamma|\xi_0, \gamma_0) = p(\xi)p(\gamma). \tag{3}$$

We can note that the conditional probability $p(\xi, \gamma|\xi_0, \gamma_0)$ is independent of l since it does not depend on the surface autocorrelation function. If the correlation is investigated, then the conditional joint probability density for a Gaussian process is expressed from [6, eq. (14a)].

Substituting (3) into (2), we have

$$\begin{cases} g_W(\theta|F; l) = \mu\Lambda \times p(\xi) \\ g_S(\theta|F; l) = \dfrac{g_W(\theta|F; l)}{\displaystyle\int_{-\infty}^{\xi_0 + \mu l} p(\xi)\, d\xi} \end{cases} \tag{4}$$

with

$$\Lambda = \frac{1}{\mu} \int_\mu^\infty (\gamma - \mu) p(\gamma)\, d\gamma. \tag{4a}$$

Since the range of the denominator of $g_S(\theta|F; l)$ is [0; 1], this inverse is $[1; \infty[$, which involves $g_S(\theta|F; l) \geq g_W(\theta|F; l)$.

From (1), since $\exp(-g)$ is a decreasing function of g, we get $S_S(\theta, F) \leq S_W(\theta, F)$. Therefore, the statistical shadowing function of Smith is smaller than Wagner's, whatever the assumed uncorrelated slope and height pdf. This comes from the fact that Smith introduces a normalization function at the denominator of (2) $g_S(\theta|F; l)\,dl$ conditional probability.

We can also note that the Smith and Wagner statistical shadowing functions depend on the surface slope γ_0 and height ξ_0. For a scattering problem from a randomly rough surface, the scattering coefficient is derived from averaging the scattered electromagnetic field multiplied by its conjugate. Thus, if the electromagnetic field depends on $\{\gamma_0, \xi_0\}$, which is the case with the Kirchhoff approach, then the statistical shadowing function has to be included in the electromagnetic field, and the scattering coefficient with shadow is obtained from averaging the shadowed electromagnetic field. This method is explained in detail in [8] and [9] and applied on the Kirchoff integral. With the geometric optics approximation, [7] showed that the average shadowing function can be used as a correction of the unshadowed scattering coefficient.

The average shadowing function $S(\theta)$ is obtained from integrating the statistical shadowing function $S(\theta, F)$ over $\{\xi_0, \gamma_0\}$

$$S(\theta) = \int_{-\infty}^{\infty}\int_{-\infty}^{\infty} S(\theta, F) \times p(\xi_0, \gamma_0)\, d\xi_0\, d\gamma_0. \tag{5}$$

Substituting (4) into (1), using (5) and [5, (2.7)] leads to

$$\begin{cases} S_W = \Lambda' \times \dfrac{1-\exp(-\Lambda)}{\Lambda} \\ S_S = \Lambda' \times \dfrac{1}{\Lambda+1} \end{cases} \tag{6}$$

with

$$\Lambda' = \int_{-\infty}^{\mu} p(\gamma)\, d\gamma. \tag{6a}$$

We can see that Wagner and Smith shadowing functions $\{S_W, S_S\}$ depend on the surface slope probability density function $p(\gamma)$ of root mean square (rms) σ within $\{\Lambda, \Lambda'\}$ and on μ. According to the following inequalities (see [15, (4.2.32)]):

$$\begin{aligned} &\frac{x}{1+x} < 1 - e^{-x} < x \\ x > 0 \quad \Rightarrow \quad &\frac{1}{1+x} < \frac{1-e^{-x}}{x} < 1 \end{aligned} \tag{7}$$

we have

$$\frac{1}{1+\Lambda} < \frac{1-e^{-\Lambda}}{\Lambda} < 1 \quad \Rightarrow \quad 0 \leq S_S < S_W < \Lambda' < 1 \tag{8}$$

with $\{\Lambda > 0, \Lambda' > 0\}$. Equation (8) is in agreement with the notice on (4). For any uncorrelated process, the Smith shadowing function averaged over the surface slopes and heights is then smaller than Wagner's.

To illustrate the above results, this paper examines the one-dimensional Gaussian (index G), Laplacian (index L), and exponential [4] (index E) surface slope pdfs with zero mean value expressed as follows:

$$\begin{cases} p_G(\gamma) = \dfrac{1}{\sigma\sqrt{2\pi}} \exp\left(-\dfrac{\gamma^2}{2\sigma^2}\right) \\ p_L(\gamma) = \dfrac{1}{\sigma\sqrt{2}} \exp\left(-\dfrac{|\gamma|\sqrt{2}}{\sigma}\right) \\ p_E(\gamma) = \dfrac{3|\gamma|}{\pi\sigma^2} K_1\left(\dfrac{\sqrt{3}|\gamma|}{\sigma}\right) \end{cases} \tag{9}$$

where $K_1(\cdots)$ is one of the modified Bessel functions of order one. $p_E(\gamma)$ is obtained from performing the marginal probability of a two-dimensional isotropic exponential distribution defined as [4]

$$p_E(\gamma) = \frac{3}{2\pi\sigma^2}\int_{-\infty}^{\infty} \exp\left[-\frac{\sqrt{3\,(\gamma^2+\gamma_1^2)}}{\sigma}\right] d\gamma_1. \tag{10}$$

We can note that the variances of $p_{G,L,E}(\gamma)$ are equal to $\langle \gamma^2 \times p_{G,L,E}(\gamma)\rangle = \sigma^2$. Comparing [4, (13)] with (9), the number six is replaced by three since the variance of $p_E(\gamma)$ has to be equal to σ^2 instead of $\sigma^2/2$.

In Fig. 2, Gaussian, Laplacian, and exponential surface slope distributions are plotted versus the slope γ with $\sigma = 1$. It should be noted that the Laplacian density shows a much greater probability of occurrence of small slopes than the Gaussian and the exponential densities. We see that the deviation between the Laplacian and exponential densities is smaller than the deviation obtained when a Gaussian density is considered.

Substituting (9) into (6) and performing the integration over the slopes γ, the parameters $\{\Lambda, \Lambda'\}$ are given in Table I according to $\nu = \mu/(\sigma\sqrt{2})$. "erfc" denotes the complementary error function. With an exponential distribution, the integration over x is computed numerically.

In Fig. 3(a), the Wagner and Smith one-dimensional monostatic shadowing functions are represented versus ν for Gaussian, Laplacian, and exponential slope distributions. In Fig. 3(b), their difference is plotted according to the Smith average shadowing function with a Gaussian slope pdf. For grazing angles corresponding to $\nu \to 0$, the shadow tends toward zero, whereas for normal angles $\nu \geq 2$, it converges to one, because the surface is entirely illuminated. For values of $\nu \leq 1$, with Laplacian and exponential distributions, the shadow is larger than that obtained with a Gaussian, whereas for $\nu > 1.2$, the contrary effect is observed. In each case, the shadow estimated with Wagner formulation is greater than that computed with Smith, which is in agreement with (8), and the deviation between the Laplacian and exponential results is small. In fact, as shown in the next section, Wagner's results are overestimated.

B. Comparison With the Numerical Shadowing Function or Exact Shadowing Function

The Smith and Wagner approaches assume that the correlation between the slopes and the heights is negligible. References [5] and [6] have introduced the correlation with Gaussian surface pdf for any surface height autocorrelation function. They compare the results with and without correlation with the nu-

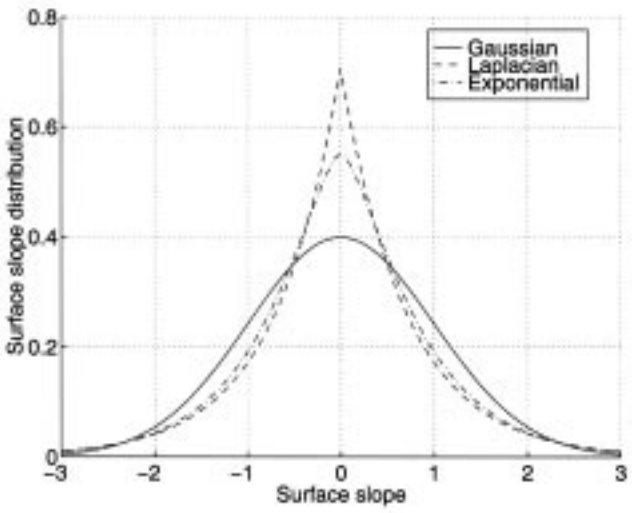

Fig. 2. Gaussian, Laplacian, and exponential slope surface pdfs with $\sigma = 1$.

TABLE I
PARAMETERS $\{\Lambda, \Lambda'\}$ FOR A ONE-DIMENSIONAL SURFACE GAUSSIAN, LAPLACIAN, AND EXPONENTIAL SLOPE PROBABILITY DENSITY FUNCTIONS IN THE MONOSTATIC CASE

	Λ	Λ'
Gaussian	$\frac{\exp(-v^2) - v\sqrt{\pi}erfc(v)}{2v\sqrt{\pi}}$	$1 - \frac{erfc(v)}{2}$
Laplacian	$\frac{\exp(-2v)}{4v}$	$1 - \frac{\exp(-2v)}{2}$
Exponential	$\sqrt{\frac{2}{3\pi}}\frac{1}{v} - \frac{1}{2} - \frac{6v^2}{\pi} \times \int_0^1 (x-1)xK_1(xv\sqrt{6})dx$	$\frac{1}{2} + \frac{6v^2}{\pi} \times \int_0^1 xK_1(xv\sqrt{6})dx$

merical solution for several surface height autocorrelation functions and show that the discrepancy between the correlated and uncorrelated curves is small. This is due to the fact that the shadowing function with correlation varies weakly with the autocorrelation function.

To compare the Wagner and Smith shadowing functions given by (6) with the numerical solution (obtained from [6, Fig. 4]), the height and slope surfaces have to be generated. For any surface height autocorrelation function, when the surface elevation pdf is Gaussian, the linearity of the filter leads also to a Gaussian surface slope pdf. The variable transformation between Laplacian-exponential $\{\gamma_L, \gamma_E\}$ and Gaussian γ_G random variables therefore has to be determined. Because it is easy to simulate numerically a Gaussian white noise, so from [16] the solution is found by solving the following differential equation:

$$p_G(\gamma_G)\, d\gamma_G = p_L(\gamma_L)\, d\gamma_L. \tag{11}$$

The exponential case is not treated because there is no analytical solution. Solving the above differential equation, this problem could be studied numerically. But the numerical errors could affect the profile of the slope pdf, involving a numerical error on the numerical solution computation of the average shadowing function, since it is very sensitive with respect to the surface slope distribution.

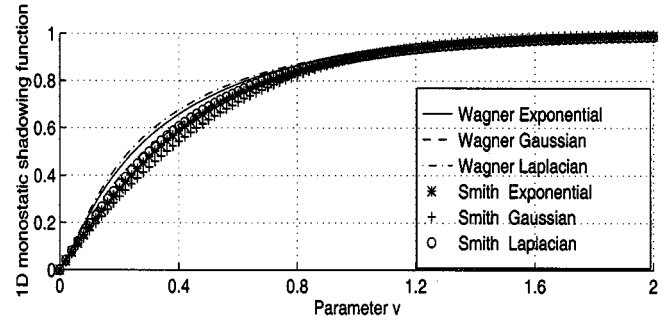

(a)

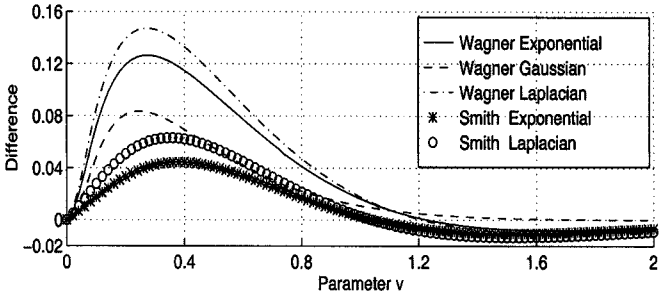

(b)

Fig. 3. (a) One-dimensional monostatic shadowing function versus $\nu = \cot\theta/(\sigma\sqrt{2})$ for Gaussian, Laplacian, and exponential slope surface distributions. (b) Difference according to the Smith average shadowing function with a Gaussian slope pdf.

Substituting (9) into (11), we get

$$\frac{1}{\sqrt{\pi}} \exp\left(-\frac{\gamma_G^2}{2\sigma^2}\right) d\gamma_G = \exp\left(-\frac{|\gamma_L|\sqrt{2}}{\sigma}\right) d\gamma_L \tag{12}$$

with $\gamma_L = f(\gamma_G)$. For $\gamma_L \geq 0$, the integration of both sides of (12) leads to

$$\text{erf}\left(\frac{\gamma_G}{\sigma\sqrt{2}}\right) = 1 - \exp\left(-\frac{\gamma_L\sqrt{2}}{\sigma}\right) \tag{13}$$

with "erf" the error function. Thus

$$\gamma_L = -\frac{\sigma}{\sqrt{2}} \ln\left[1 - \text{erf}\left(\frac{\gamma_G}{\sigma\sqrt{2}}\right)\right] \qquad \text{if } \gamma_L \geq 0. \tag{14}$$

The condition $\gamma_L \geq 0$ involves $\gamma_G \geq 0$. For $\gamma_L < 0$, the use of the same way as previously leads to

$$\begin{cases} \gamma_L = -\dfrac{\sigma}{\sqrt{2}} \ln\left[1 - erf\left(\dfrac{\gamma_G}{\sigma\sqrt{2}}\right)\right] & \text{with } \gamma_G \geq 0 \\ \gamma_L = \dfrac{\sigma}{\sqrt{2}} \ln\left[1 + erf\left(\dfrac{\gamma_G}{\sigma\sqrt{2}}\right)\right] & \text{with } \gamma_G < 0. \end{cases} \tag{15}$$

As shown in Fig. 4(a), the first step is to simulate a Gaussian white noise $b(i)$ (100 000 samples) of variance one with zero mean value (centered on zero). We see a good agreement between the theoretical and numerical results. As depicted in Fig. 4(b), a white noise is characterized by a Dirac autocorrelation function.

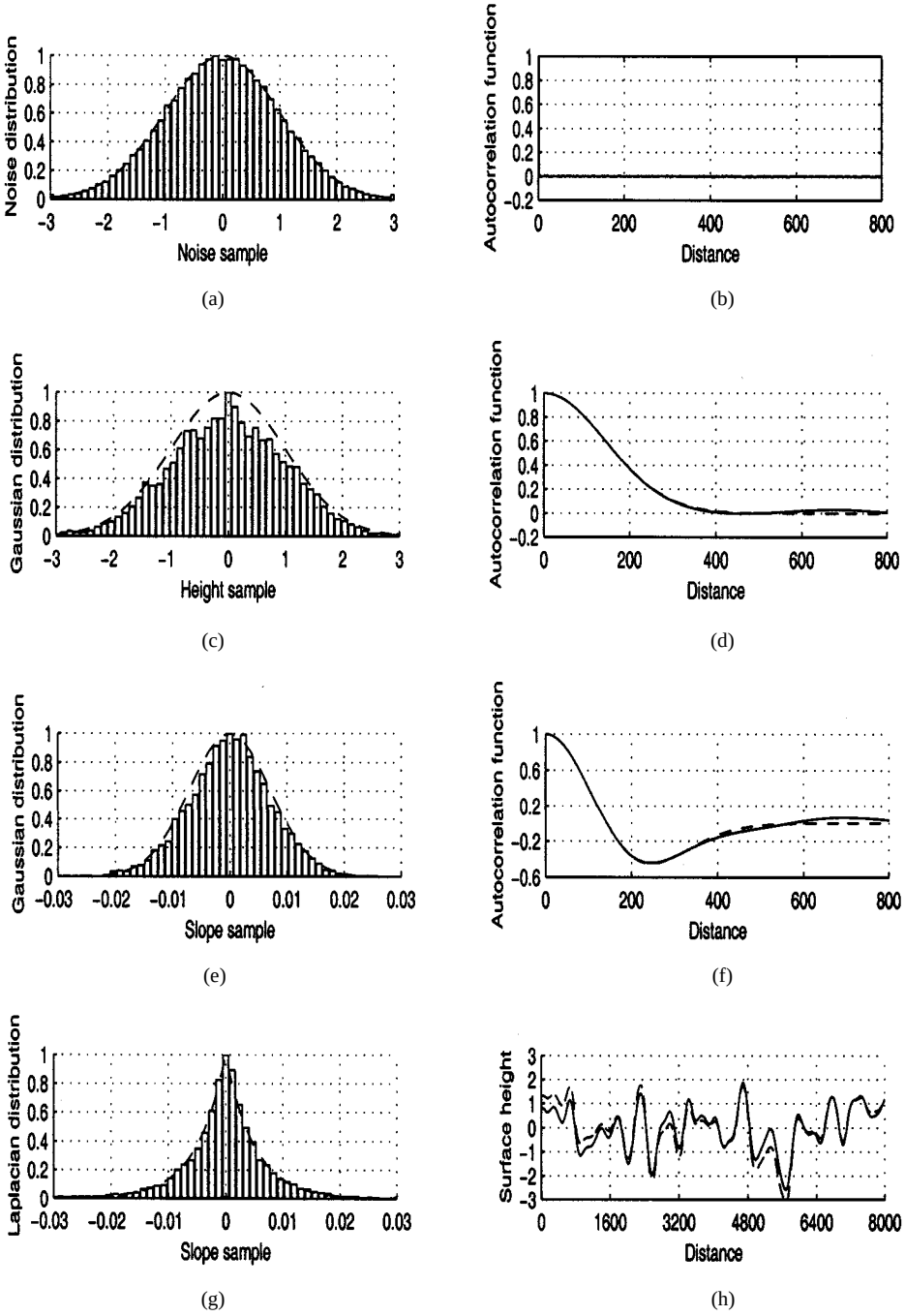

Fig. 4. Statistical properties of the height and slope surfaces of a Gaussian surface height autocorrelation function with a Gaussian height distribution. The length correlation is $L_c = 200$ and the number of samples is 100 000.

The second step is to simulate a Gaussian height surface with a surface height autocorrelation function $R_0(l)$ assumed to be Gaussian

$$R_0(l) = \omega^2 \times \exp\left(-\frac{l^2}{L_c^2}\right) \tag{16}$$

with L_c the surface correlation length and ω^2 the surface height variance. From [6], the height samples $z(i)$ are computed by writing that

$$z(i) = b(i) * w(i). \tag{17}$$

The symbol $*$ is the convolution product. $w(i)$ denotes the filter coefficients, equal for a Gaussian autocorrelation function [6]

$$w(i) = \omega\sqrt{\frac{2}{L_C\sqrt{\pi}}}\exp\left(-\frac{2i^2}{L_C^2}\right). \tag{18}$$

From Fig. 4(d), the surface height autocorrelation function is well Gaussian with $L_C = 200$. As depicted in Fig. 4(c), the linearity of the filter involves a Gaussian height histogram. From Fig. 4(e), since the height samples $z_G(i)$ are Gaussian represented in Fig. 4(c), the slope samples $\gamma_G(i) = dz_G(i)/di$ equal

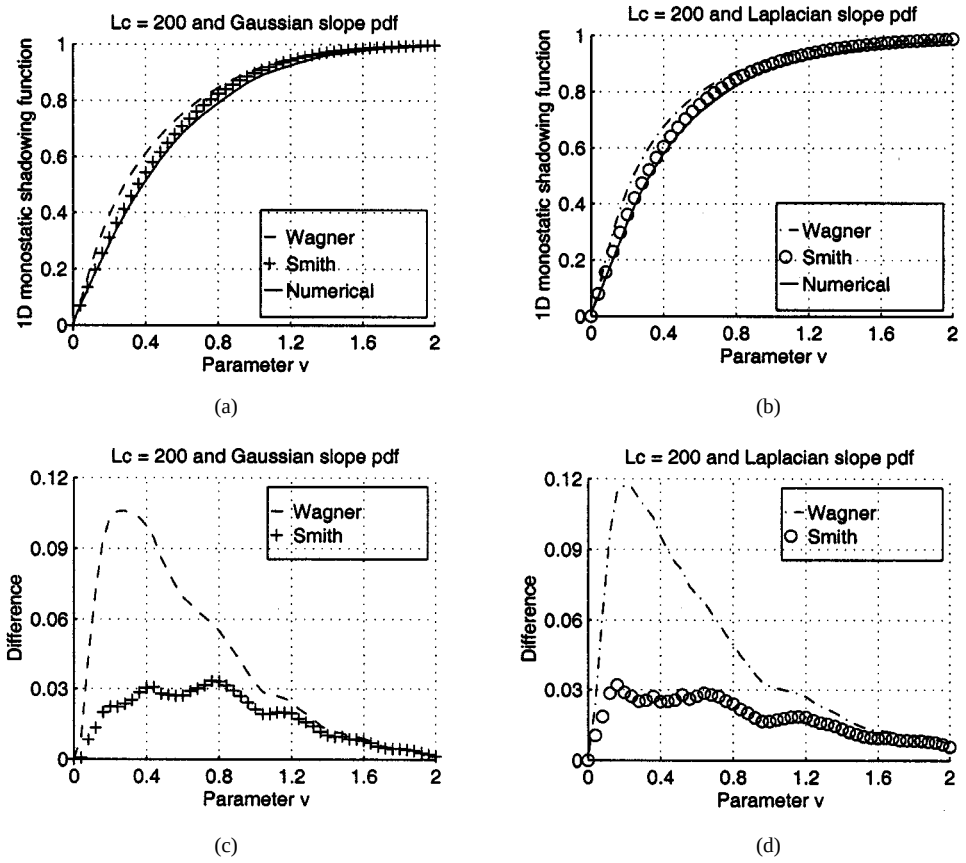

Fig. 5. (a) and (b) One-dimensional monostatic shadowing function versus $\nu = \cot\theta/(\sigma\sqrt{2})$ for a Gaussian surface height pdf with Gaussian and Laplacian surface slope pdfs, $L_C = 200$. (c) and (d) Difference between the Smith and Wagner shadowing functions according to the numerical solution.

to $z_G(i+1) - z_G(i)$ are also Gaussian, and the surface slope autocorrelation function $R_2(l)$ is theoretically

$$R_2(l) = -\frac{d^2R_0}{dl^2} = \frac{2\omega^2}{L_C^2}\left(\frac{2l^2}{L_C^2} - 1\right)\exp\left(-\frac{l^2}{L_C^2}\right) \tag{19}$$

with a surface slope variance σ^2 given by

$$\sigma^2 = -R_2(0) = \frac{2\omega^2}{L_C^2}. \tag{20}$$

Fig. 4(f) shows a very good agreement between the theoretical and numerical surface slope autocorrelation functions. Note that $\sigma = 0.00700$, computed numerically, is close to the theoretical value equal to 0.00707.

As shown in Fig. 4(g), for the last step, we apply (15) for computing the samples $\gamma_L(i)$ of a Laplacian surface slope pdf. Knowing $\gamma_L(i)$, the surface height $z_L(i)$ is built by writing

$$z_L(i) = \sum_{j=1}^{i} \gamma_L(j). \tag{21}$$

In Fig. 4(h), the height samples $\{z_G(i), z_L(i)\}$ are plotted. In conclusion, they have the same height variance $\omega = 0.9865$ (theoretical value is one) with the same Gaussian height pdf [Fig. 4(c)], but their slope pdf is different [Fig. 4(e) and (g)]. From the surfaces $\{z_G(i), z_L(i)\}$, the numerical shadowing functions are evaluated by using the algorithm described in [6, Fig. 4].

In Figs. 5(a) and (b) and 6(a) and (b), the Wagner, Smith, and numerical monostatic one-dimensional shadowing functions are compared versus ν, with $L_C = \{100, 200\}$ and 100 000 samples. In parts (c) and (d) are plotted the differences of the Wagner and Smith shadowing function according to the numerical solution. In Table II, the values of the shadowing function are given, with a surface rms slope $\sigma = 0.3$, $\theta = 75.7°$ leading $\nu = \cot\theta/(\sigma\sqrt{2}) = 0.6$. We see with the Smith approach that the results are more accurate than those obtained with the Wagner approach, and the discrepancy between the numerical and Smith data is small. In both cases, the shadowing effect is overestimated. Thus, the Smith approach is kept as a comparison in this paper.

References [5] and [6], with a Gaussian surface height and slope joint pdf and for different surface height autocorrelation functions, proved that including the correlation between the heights and the slopes slightly improves the shadowing function.

III. One-Dimensional Surface for a Bistatic Configuration

This section presents the bistatic shadowing function for a one-dimensional rough surface. Since the results obtained with the Smith formulation are more accurate than Wagner's formulation, only the Smith approach is kept in the following.

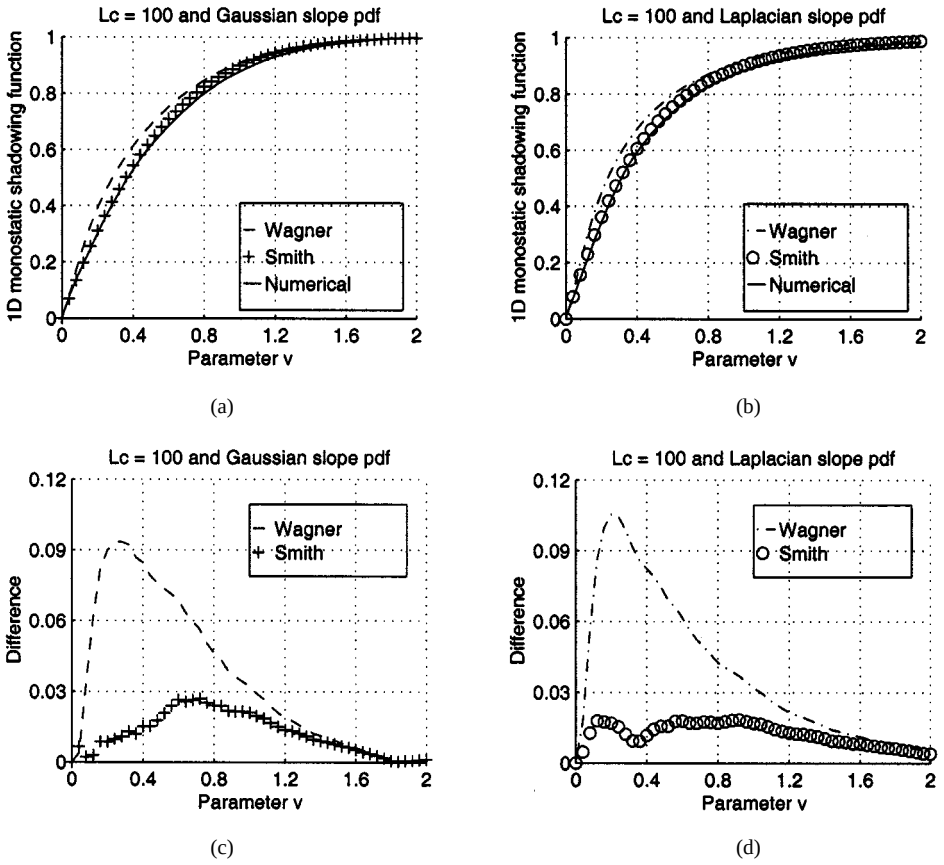

Fig. 6. Same variation as Fig. 5 with $L_C = 100$.

TABLE II
VALUES OF THE SHADOW FOR $\nu = \cot\theta/(\sigma\sqrt{2}) = 0.6$

	Wagner	Smith	Numerical
Gaussian	0.752	0.701	0.683
Laplacian	0.798	0.755	0.723

From [5, (2.31)], the statistical bistatic shadowing function is given by

$$S(\theta_1, \theta_2, F) = \begin{cases} S(\theta_1, F)S(\theta_2, F), & \text{if } \theta_2 \in [0; \pi/2] \quad \text{case a)} \\ S(\theta_1, F), & \text{if } \theta_2 \in [\theta_1; 0[\quad \text{case b)} \\ S(\theta_2, F), & \text{if } \theta_2 \in [-\pi/2; \theta_1[\quad \text{case c)} \end{cases} \tag{22}$$

with $\theta_1 \leq 0$. Equation (22) involves that the statistical bistatic shadowing function $S(\theta_1, \theta_2, F)$ is obtained from two independent statistical monostatic shadowing functions defined with respect to the locations of the transmitter $S(\theta_1, F)$ and the receiver $S(\theta_2, F)$. Consequently, the b) and c) cases are similar to the monostatic configuration, and case a) has to be investigated.

Substituting (3) and (2) into (1), the Smith a) case of (22) is expressed as

$$S_S(\theta_1, F) \times S_S(\theta_2, F) = \Upsilon(|\mu_1| + \gamma_0) \times \Upsilon(\mu_2 - \gamma_0) \times \exp\left\{ - \int_0^{\infty} p(\xi) \left[\frac{\int_{|\mu_1|}^{\infty} (\gamma - |\mu_1|) \times p(\gamma)\, d\gamma}{\int_{-\infty}^{\infty} p(\gamma)\, d\gamma \int_{-\infty}^{\xi_0 + |\mu_1| l} p(\xi)\, d\xi} + \frac{\int_{\mu_2}^{\infty} (\gamma - \mu_2) \times p(\gamma)\, d\gamma}{\int_{-\infty}^{\infty} p(\gamma)\, d\gamma \int_{-\infty}^{\xi_0 + \mu_2 l} p(\xi)\, d\xi} \right] dl \right\}. \tag{23}$$

Since the transmitter is defined for $y < 0$, the sign of γ_0 in $\Upsilon(|\mu_1| + \gamma_0)$ is positive and the slope $\mu_1 = \cot\theta_1$ of the incident ray becomes $|\mu_1|$. The use of (4a) leads to

$$S_S(\theta_1, F) \times S_S(\theta_2, F) = \Pi \times \exp\left\{ - \int_0^{\infty} p(\xi) \left[\frac{\Lambda_1 \times |\mu_1|}{\int_{-\infty}^{\xi_0 + |\mu_1| l} p(\xi)\, d\xi} + \frac{\Lambda_2 \times \mu_2}{\int_{-\infty}^{\xi_0 + \mu_2 l} p(\xi)\, d\xi} \right] dl \right\} \tag{24}$$

with $\{\Lambda_1 = \Lambda(|\mu_1|), \Lambda_2 = \Lambda(\mu_2)\}$, and $\Pi = \{1 \text{ if } \gamma_0 \in [-|\mu_1|, \mu_2] \text{ else } 0\}$. Using the following variable transforma-

tions $\{\xi' = \xi_0 + |\mu_1| l,\ \xi' = \xi_0 + \mu_2 l\}$ for each integral over l, we get

$$S_S(\theta_1, F) \times S_S(\theta_2, F) = \Pi \times \exp\left\{-(\Lambda_1 + \Lambda_2) \times \int_{\xi_0}^{\infty} \left[\frac{p(\xi')}{\int_{-\infty}^{\xi'} p(\xi)\, d\xi}\right] d\xi'\right\}. \quad (25)$$

Let P be a primitive of $p(\xi')$

$$P = \int p(\xi')\, d\xi'$$

$$\Rightarrow \int_{\xi_0}^{\infty} \frac{dP(\xi')}{P(\xi') - P(-\infty)} = -\ln|P(\xi_0) - P(-\infty)| \quad (25a)$$

because $P(\infty) - P(-\infty) = 1$. We obtain

$$\begin{aligned} &S_S(\theta_1, F) \times S_S(\theta_2, F) \\ &\quad = \Pi \times \exp\left\{-(\Lambda_1 + \Lambda_2) \times \int_{\xi_0}^{\infty} \frac{dP(\xi')}{P(\xi') - P(-\infty)}\right\} \\ &\quad = \Pi \times |P(\xi_0) - P(-\infty)|^{\Lambda_1 + \Lambda_2}. \end{aligned} \quad (26)$$

Substituting (26) into (5), the Smith average bistatic shadowing function is expressed as

$$S_S(\theta_1, \theta_2) = \left[\int_{-\infty}^{\infty} |P(\xi_0) - P(-\infty)|^{\Lambda_1 + \Lambda_2} \times p(\xi_0)\, d\xi_0\right] \times \int_{-|\mu_1|}^{\mu_2} p(\gamma_0)\, d\gamma_0. \quad (27)$$

The integration over ξ_0 leads to

$$S_S(\theta_1, \theta_2) = \frac{1}{1 + \Lambda_1 + \Lambda_2} \times \int_{-|\mu_1|}^{\mu_2} p(\gamma_0)\, d\gamma_0. \quad (28)$$

Writing that

$$\begin{aligned} \int_{-\infty}^{\infty} p(\gamma_0)\, d\gamma_0 &= 1 \\ &= \int_{-\infty}^{|\mu_2|} p(\gamma_0)\, d\gamma_0 + \int_{-\infty}^{\mu_2} p(\gamma_0)\, d\gamma_0 \\ &\quad - \int_{-|\mu_1|}^{\mu_2} p(\gamma_0)\, d\gamma_0. \end{aligned} \quad (29)$$

From (6a), we have finally

$$S_S(\theta_1, \theta_2) = \frac{\Lambda_1' + \Lambda_2' - 1}{1 + \Lambda_1 + \Lambda_2} \quad (30)$$

with $\{\Lambda_1' = \Lambda'(|\mu_1|)$ and $\Lambda_2' = \Lambda'(\mu_2)\}$. Since b) and c) of (22) are monostatic cases, the Smith average bistatic shadowing function is expressed as

$$S_S(\theta_1, \theta_2) = \frac{\Lambda_b'}{1 + \Lambda_b}$$

with
$$\begin{cases} \{\Lambda_b' = \Lambda_1' + \Lambda_2' - 1,\ \Lambda_b = \Lambda_1 + \Lambda_2\} \\ \quad \text{if } \theta_2 \in [0;\ \pi/2] \\ \{\Lambda_b' = \Lambda_1',\ \Lambda_b = \Lambda_1\} \\ \quad \text{if } \theta_2 \in [\theta_1;\ 0[\\ \{\Lambda_b' = \Lambda_2',\ \Lambda_b = \Lambda_2\} \\ \quad \text{if } \theta_2 \in [-\pi/2;\ \theta_1[. \end{cases} \quad (31)$$

We can note for the a) case that $S_S(\theta_1, \theta_2) \neq S_S(\theta_1) \times S_S(\theta_2)$. The form of (31) is similar to (6) with new values of $\{\Lambda, \Lambda'\}$. With the Wagner approach, we can show that the form is also similar.

Using equations of Table I for Gaussian, Laplacian, and exponential surface slope distributions, the functions $\{\Lambda_b, \Lambda_b'\}$ are expressed with respect to

$$\nu_i = \frac{\cot|\theta_i|}{\sigma\sqrt{2}}. \quad (31a)$$

Equation (31) then becomes

$$S_S(\nu_1, \nu_2) = \frac{\Lambda_b'}{1 + \Lambda_b}$$

with
$$\begin{cases} \{\Lambda_b' = \Lambda_1' + \Lambda_2' - 1,\ \Lambda_b = \Lambda_1 + \Lambda_2\} \\ \quad \text{if } \nu_2 \geq 0 \\ \{\Lambda_b' = \Lambda_1',\ \Lambda_b = \Lambda_1\} \\ \quad \text{if } -\nu_1 \leq -\nu_2 < 0 \\ \{\Lambda_b' = \Lambda_2',\ \Lambda_b = \Lambda_2\} \\ \quad \text{if } -\infty \leq -\nu_2 < -\nu_1. \end{cases} \quad (32)$$

Applying the same approach as the monostatic case, in Fig. 7(a) and (b), the Smith bistatic shadowing function is compared with the numerical one versus the parameter ν_2, with $|\nu_1| = \{0.4,\ 1.2\}$, for Gaussian and Laplacian slopes, whereas the height surface is Gaussian, $L_C = 200$. The height and slope surfaces are the same as in Fig. 4. In Fig. 7(c) and (d), the difference between the Smith and numerical solutions is plotted. As shown, Smith's results are weakly overestimated, and this overestimation increases when $|\nu_1|$ decreases.

IV. Two-Dimensional Shadowing Function

From [5], which has treated only the Gaussian process, in this section the Smith one-dimensional shadowing function is extended to two-dimensional surfaces. At first, with a Gaussian process and for a monostatic configuration, the method is exposed and applied to a Laplacian process. The last subsection extends the model to a bistatic configuration for both processes. This point is very relevant, because in the literature, except [5], the surface is assumed to be either one-dimensional or isotropic.

The numerical solution of the average shadowing function cannot be treated because it requires the generation of a two-dimensional surface. To have a good representation of the surface statistics such as the surface height autocorrelation function and its distribution, an important number of surface samples

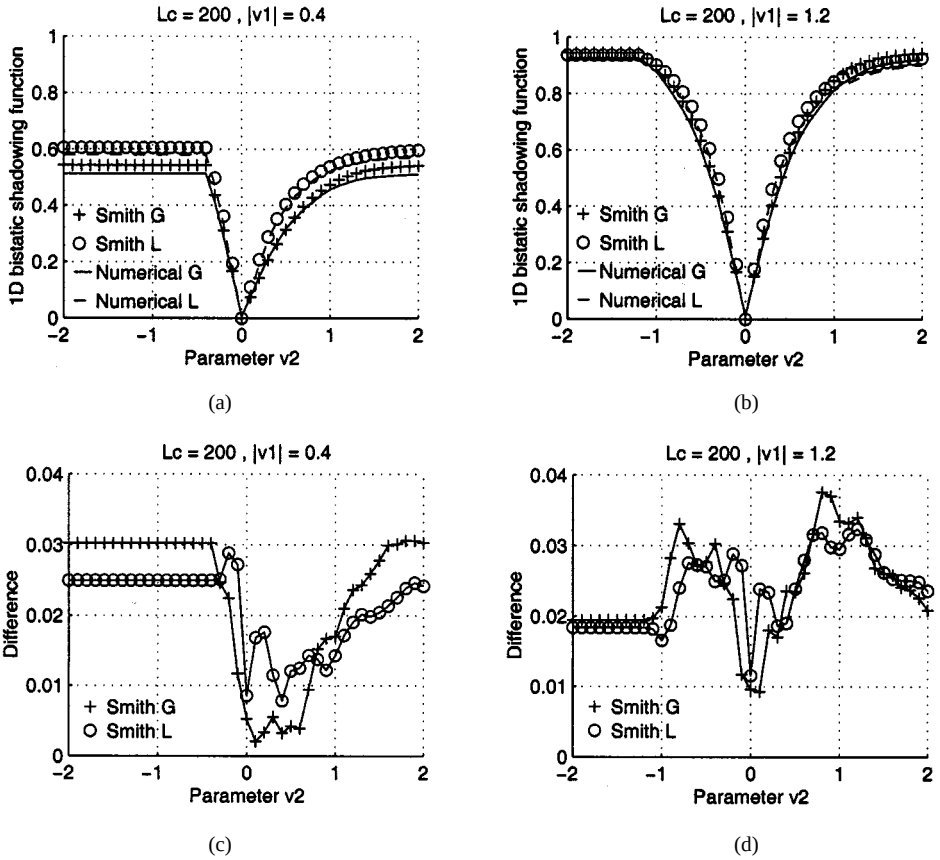

Fig. 7. (a) and (b) One-dimensional bistatic shadowing function versus $\nu_2 = \cot|\theta_2|/(\sigma\sqrt{2})$ with $|\nu_1| = \{0.4,\ 1.2\}$, for a Gaussian surface height pdf with Gaussian and Laplacian surface slope pdfs, $L_C = 200$. (c) and (d) Difference between the Smith and numerical solutions.

is required. With a one-dimensional surface, we have chosen $N = 100\,000$, which implies that with a two-dimensional surface, we have to generate a matrix Gaussian white noise $B(i)$ of dimension $N \times N$. From (17), the convolution product with the filter coefficients also has to be computed. To improve the computer time, we could make this operation in the Fourier domain and use an algorithm of fast Fourier transform, but the size of the memory remains insufficient. Moreover, since the Fourier transform is valid in Cartesian coordinates and the shadowing function is expressed in polar coordinates, the surface cross-section in the azimuthal direction ϕ has to be evaluated.

A. Monostatic Configuration

For a two-dimensional surface, the slope pdf $p_G(\gamma_x, \gamma_y)$, assumed to be Gaussian, is expressed as follows:

$$p_G(\gamma_x, \gamma_y) = \frac{1}{2\pi\sqrt{|[C]|}} \exp\left(-\frac{1}{2}\,[\gamma_x \ \ \gamma_y][C]^{-1}\begin{bmatrix}\gamma_x\\ \gamma_y\end{bmatrix}\right) \tag{33}$$

with

$$[C] = \begin{bmatrix}\sigma_x^2 & \sigma_{xy}^2\\ \sigma_{xy}^2 & \sigma_y^2\end{bmatrix} \tag{33a}$$

where $\{\gamma_x, \gamma_y\}$ denote the surface slopes of variance $\{\sigma_x^2, \sigma_y^2\}$ in the $\{(Ox), (Oy)\}$ directions (Fig. 8), respectively. $[C]$ is the covariance matrix of determinant $|[C]|$. To have a real surface without an imaginary part, its spectrum has to be Hermitian, which involves that the autocorrelation function $R_0(x, y)$ obtained from the inverse Fourier transform of the spectrum is even according to $\{(Ox), (Oy)\}$ directions. This means that $R_0(x, y)$ depends on $\{X = x^2, Y = y^2\}$. The "even" may be obtained with $\{X = |x|, Y = |y|\}$, but $R_0(x, y)$ is not derivable at zero. Therefore, the surface cross-variance σ_{xy}^2 is equal to zero, since it is equal to

$$\sigma_{xy}^2 = \frac{\partial^2}{\partial x\,\partial y}\left[-R_0\left(x^2, y^2\right)\right]\Big|_{\substack{x=0\\ y=0}} = 0. \tag{34}$$

Consequently, (33) becomes

$$p_G(\gamma_x, \gamma_y) = \frac{1}{2\pi\sigma_x\sigma_y}\exp\left(-\frac{\gamma_x^2}{2\sigma_x^2} - \frac{\gamma_y^2}{2\sigma_y^2}\right). \tag{35}$$

With Laplacian and exponential two-dimensional surface slope probability density functions, we get

$$p_L(\gamma_x, \gamma_y) = \frac{1}{2\sigma_x\sigma_y}\exp\left(-\frac{|\gamma_x|\sqrt{2}}{\sigma_x} - \frac{|\gamma_y|\sqrt{2}}{\sigma_y}\right) \tag{36}$$

$$p_E(\gamma_x, \gamma_y) = \frac{3}{2\pi\sigma_x\sigma_y}\exp\left[-\sqrt{3\left(\frac{\gamma_x^2}{\sigma_x^2} + \frac{\gamma_y^2}{\sigma_y^2}\right)}\right]. \tag{37}$$

The two-dimensional shadowing function is characterized in polar coordinates by the azimuth angle ϕ [observation direction according to (Ox)] and the incidence angle θ (Fig. 8). For a constant direction ϕ, the issue is one-dimensional. The idea [5]

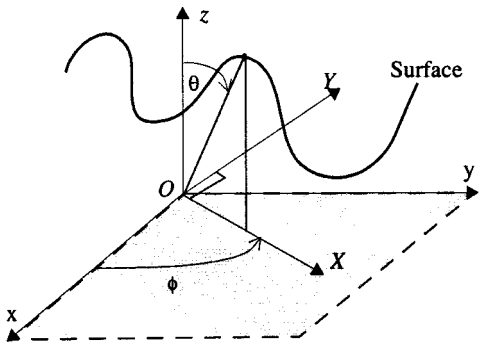

Fig. 8. Two-dimensional configuration.

is to extend the one-dimensional results to the two-dimensional surface by executing a rotation of an angle ϕ around the (Oz) axis.

To determine the slope probability density $p(\gamma_X, \gamma_Y)$ in the direction ϕ, we make a base transformation (X, Y, z). The former coordinates $\{\gamma_x, \gamma_y\}$ are expressed by the new ones $\{\gamma_X, \gamma_Y\}$ as

$$\begin{cases} \gamma_x = \gamma_X \cos\phi - \gamma_Y \sin\phi \\ \gamma_y = \gamma_X \sin\phi + \gamma_Y \cos\phi \end{cases} \tag{38}$$

with $\{\gamma_X, \gamma_Y\}$ the surface slopes in the $\{(OX), (OY)\}$ directions (Fig. 8). Substituting (38) into (35), the marginal probability $p(\gamma_X)$ defined as

$$p(\gamma_X) = \int_{-\infty}^{\infty} p(\gamma_X, \gamma_Y)\, d\gamma_Y \tag{39}$$

is then equal for a Gaussian process to [5, 2.41]

$$p_G(\gamma_x) = \frac{1}{\sigma_X \sqrt{2\pi}} \exp\left(-\frac{\gamma_X^2}{2\sigma_X^2}\right) \tag{40}$$

with

$$\sigma_X^2 = (\sigma_x \cos\phi)^2 + (\sigma_y \sin\phi)^2. \tag{40a}$$

The marginal probability $p_G(\gamma_X)$ in the direction ϕ is also a Gaussian function with variance σ_X^2. Consequently, for a monostatic configuration with a Gaussian slope pdf, the two-dimensional shadowing function is obtained from the one-dimensional shadowing function by replacing in (4a) and (6a) σ by $\sigma_X(\phi)$.

Substituting (36) and (38) into (39) and performing the integration over γ_X, we show with a Laplacian slope pdf that the marginal probability $p_L(\gamma_X)$ is

$$p_L(\gamma_X) = \frac{u_c \exp\left(-\dfrac{|\gamma_X|\sqrt{2}}{u_c}\right) - u_s \exp\left(-\dfrac{|\gamma_X|\sqrt{2}}{u_s}\right)}{\sqrt{2}(u_c^2 - u_s^2)} \tag{41}$$

with

$$u_c = \sigma_x \cos\phi \qquad u_s = \sigma_y \sin\phi. \tag{41a}$$

We can verify that $E_L(\gamma_X^2) = E_G(\gamma_X^2) = \sigma_X^2$, with $E(\cdots)$ the expected value. Since the marginal probability is not exponential as (9), $\{\Lambda, \Lambda'\}$ has to be performed from (4a) and (6a) with $\gamma = \gamma_X$, and we show (42) at the bottom of the page.

Since the integration over γ_X is impossible with an exponential surface slope pdf, its marginal probability is not performed, and the Gaussian and Laplacian profiles are only studied.

In Fig. 9, the Smith monostatic two-dimensional shadowing function is plotted versus $\{\phi, \theta\}$ in degrees with Gaussian and Laplacian slope distributions. As shown in Fig. 9(a) and (b), with $\{\sigma_x = 0.3, \sigma_y = 0.25\}$, the shadow increases weakly with ϕ and increases with θ, because the ratio of illuminated surface decreases. As the one-dimensional surface (Fig. 3), the shadow with a Laplacian process is slightly larger than that obtained with a Gaussian process. From Fig. 9(c) and (d) with $\{\sigma_x = 0.3, \sigma_y = 0.20\}$, when the shadow is close to one, the contrary effect is observed. Since σ_y is smaller than Fig. 9(a) and (b), the anisotropic effect is more important. Comparing Fig. 9(e) and (f) for $\{\sigma_x = 0.25, \sigma_y = 0.20\}$ with Fig. 9(c) and (d), the shadowing function is greater because the surface rms slope is smaller.

B. Bistatic Configuration

Since with a Gaussian surface slope pdf the marginal probability remains Gaussian with a variance σ_X^2 given by (40a), the bistatic configuration is obtained from the substitution of ν_i in (31a) by

$$\nu_i = \frac{\cot|\theta_i|}{\sqrt{2}\sigma_X(\phi_i)} \tag{43}$$

where $\{\phi_1, \phi_2\}$ denote the transmitter and receiver azimuthal directions, respectively, and θ_i their incidence angles. Substituting ν_i into (32), the Smith two-dimensional bistatic shadowing function is calculated with respect to $\{\theta_i, \phi_i; \sigma_x, \sigma_y\}$.

$$\begin{cases} \Lambda_L = \dfrac{u_c^3 \exp\left(-\dfrac{\mu\sqrt{2}}{u_c}\right) - u_s^3 \exp\left(-\dfrac{\mu\sqrt{2}}{u_s}\right)}{2\sqrt{2}\mu(u_c^2 - u_s^2)} \\ \Lambda_L' = \dfrac{u_c^2\left[1 - \dfrac{1}{2}\exp\left(-\dfrac{\mu\sqrt{2}}{u_c}\right)\right] - u_s^2\left[1 - \dfrac{1}{2}\exp\left(-\dfrac{\mu\sqrt{2}}{u_s}\right)\right]}{(u_c^2 - u_s^2)}. \end{cases} \tag{42}$$

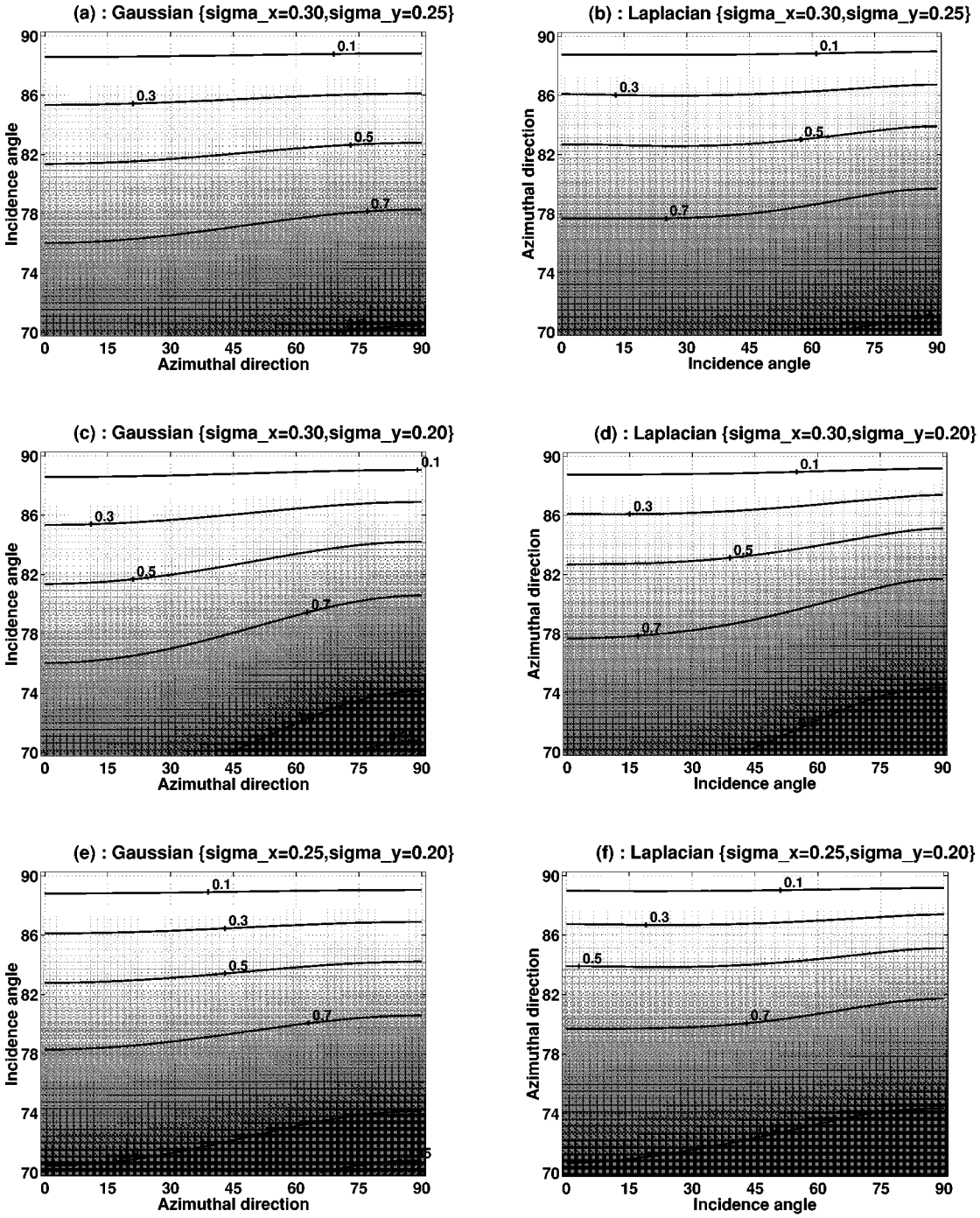

Fig. 9. Two-dimensional monostatic shadowing function with Gaussian and Laplacian slope pdfs.

With a Laplacian surface slope pdf, the Smith two-dimensional bistatic shadowing function is computed from (32) and (42), where $\{\mu = \cot\theta,\, u_c = \sigma_x \cos\phi,\, u_s = \sigma_y \sin\phi\}$ is replaced by $\{|\mu_i| = \cot\theta_i,\, u_c = \sigma_x \cos\phi_i,\, u_s = \sigma_y \sin\phi_i\}$ according to the transmitter $(i = 1)$ or the receiver $(i = 2)$.

In Fig. 10, the Smith two-dimensional bistatic shadowing function is plotted versus the location of the receiver $\{\theta_2, \phi_2\}$ for fixed location of the transmitter $\theta_1 = 70°$ and $\phi_1 = \{0, 90\}°$. The surface rms slopes are $\sigma_x = 0.3$, $\sigma_y = 0.2$ with Gaussian [Fig. 10(a)–(c)] and Laplacian [Fig. 10(b)–(d)] surface slope probability density functions. We can note that the shadowing function increases with ϕ_1 because the surface variance slope in the ϕ_1 direction decreases.

V. Conclusion

The shadowing theory developed by [1]–[3] is investigated in this paper for any surface height and slope uncorrelated pdf. As shown by [5] and [6], when the correlation is ignored, the statistical shadowing function does not depend on the surface height

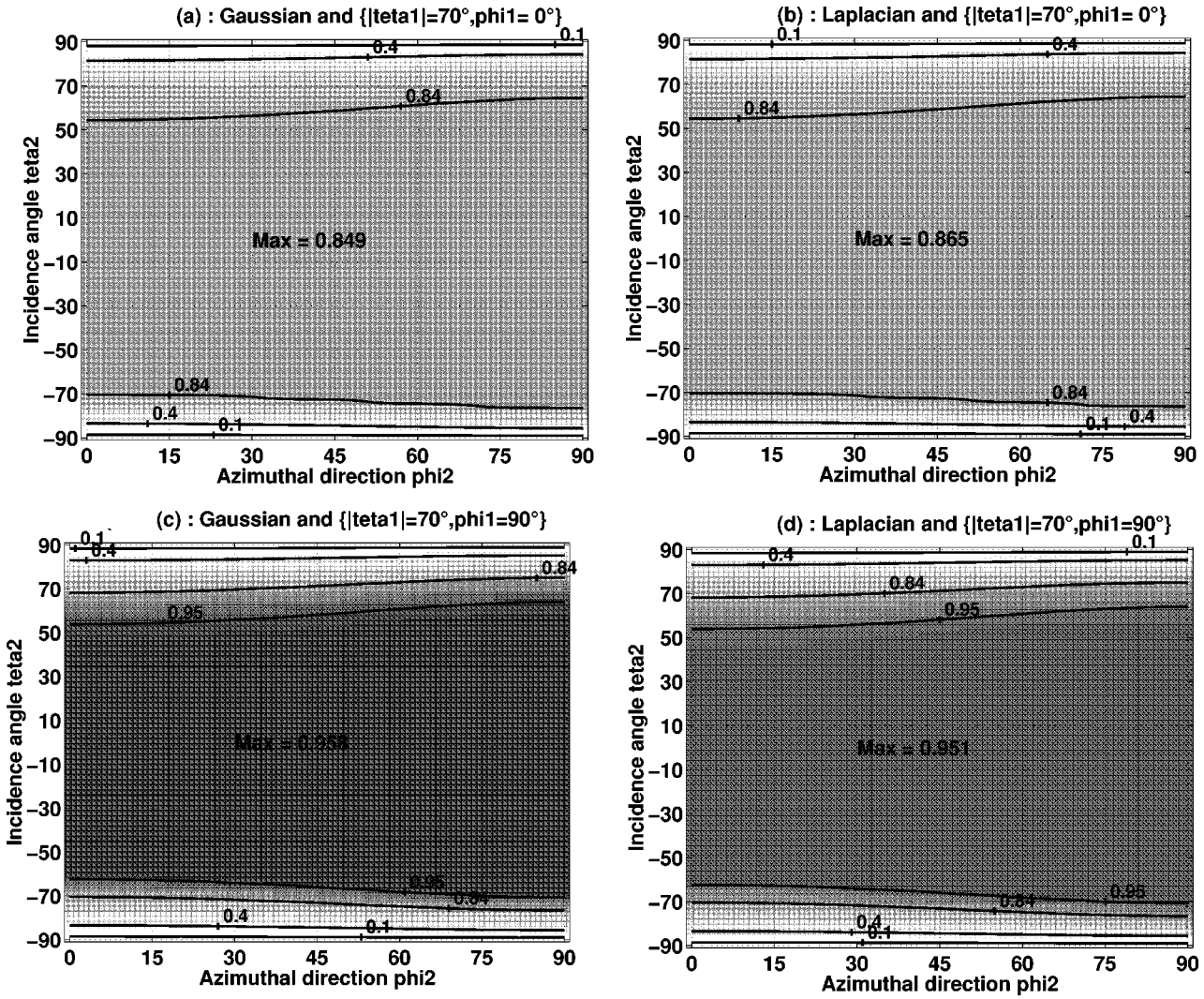

Fig. 10. Smith two-dimensional bistatic shadowing function versus the location of the receiver $\{\theta_2, \phi_2\}$ for a constant location of the transmitter $\{\theta_1, \phi_1\}$ with $\sigma_x = 0.3$ and $\sigma_y = 0.2$.

autocorrelation function. This allows a simpler shadowing function, and we show in this paper that it depends only on the surface slope pdf.

To illustrate the method with a one-dimensional surface, the average shadowing function is applied for Gaussian, Laplacian, and exponential slope distributions. The comparison of the Smith and Wagner monostatic shadowing functions with the numerical solution [13] shows that the Wagner results are overestimated, whereas the Smith results are close to the numerical solution. In fact, we show mathematically for an arbitrary surface slope pdf that the Smith statistical shadowing function is smaller than Wagner's, involving that the average is also smaller. The numerical solution [6] is obtained from generating Gaussian and Laplacian slope distributions with a Gaussian height pdf. Since it is easy to generate Gaussian samples, the relationship between Laplacian and Gaussian samples has to be determined, which is similar to solving a differential equation [16]. The method is extended to the bistatic configuration.

Considering a two-dimensional rough surface, the analysis is extended to monostatic and bistatic configurations with Gaussian and Laplacian anisotropic surface slope distributions. Therefore, in this paper, we have developped a two-dimensional shadowing function that can be used in the Kirchhoff formulation. With the geometric optics approximation, [7] proved that the shadowed scattering coefficient can be obtained from multiplying the unshadowed scattering coefficient by the average shadowing function. However, with the Kirchhoff integral, to take into account the shadowing effect, the statistical shadowing function has to be integrated in the electromagnetic field. This means that the scattering coefficient with shadow is performed by averaging the shadowed field by its conjugate. This approach is explained in detail in [8] and [9] with a Gaussian process.

ACKNOWLEDGMENT

The authors would like to thank the reviewers of this paper for their relevant comments.

REFERENCES

[1] R. J. Wagner, "Shadowing of randomly rough surfaces," *J. Opt. Soc. Amer.*, vol. 41, no. 1, pp. 138–147, June 1966.

[2] B. G. Smith, "Lunar surface roughness, shadowing and thermal emission," *J. Geophys. Res.*, vol. 72, no. 16, pp. 4059–4067, Aug. 1967.

[3] ——, "Geometrical shadowing of a random rough surface," *IEEE Trans. Antennas Propagat.*, vol. AP-15, pp. 668–671, Sept. 1967.

[4] G. S. Brown, "Shadowing by non-Gaussian random surfaces," *IEEE Trans. Antennas Propagat.*, vol. AP-28, pp. 788–790, Nov. 1980.

[5] C. Bourlier, J. Saillard, and G. Berginc, "The shadowing function," in *Progress in Electromagnetic Research*, J. A. Kong, Ed., 2000, vol. 27, pp. 226–287.

[6] ——, "Effect of correlation between shadowing and shadowed points on the Wagner and Smith monostatic one-dimensional shadowing functions," *IEEE Trans. Antennas Propagat.*, vol. 48, pp. 437–446, Mar. 2000.

[7] M. I. Sancer, "Shadow-corrected electromagnetic scattering from a randomly rough surface," *IEEE Trans. Antennas Propagat.*, vol. AP-17, pp. 577–585, Sept. 1969.

[8] C. Bourlier, G. Berginc, and J. Saillard, "Bistatic scattering coefficient from one- and two-dimensional random surfaces using the stationary phase and scalar approximation with shadowing effect—Comparisons with experiments and application to the sea surface," *Waves in Random Media*, vol. 2, no. 11, pp. 91–118, Apr. 2001.

[9] ——, "Theoretical study of the Kirchhoff integral from two-dimensional randomly rough surface with shadowing effect—Application on the backscattering coefficient for a perfectly conducting surface," *Waves in Random Media*, vol. 2, no. 11, pp. 119–147, Apr. 2001.

[10] G. T. Ruck, D. E. Barrick, W. D. Stuart, and C. K. Krichbaum, *Radar Cross Section*. New York: Plenum, 1970, vol. 2.

[11] L. M. Ricciardi and S. Sato, "On the evaluation of first passage time densities for Gaussian processes," *Signal Processing*, vol. 11, pp. 339–357, 1986.

[12] ——, "A note on first passage time problems for Gaussian processes and varying boundaries," *IEEE Trans. Inform. Theory*, vol. IT-29, May 1983.

[13] R. A. Brokelman and T. Hagfors, "Note of the effect of shadowing on the backscattering of waves from a random rough surface," *IEEE Trans. Antennas Propagat.*, vol. AP-14, pp. 621–627, Sept. 1967.

[14] D. A. Kapp and G. S. Brown, "Effect of correlation between shadowing and shadowed points in rough surface scattering," *IEEE Trans. Antennas Propagat.*, vol. 42, pp. 1154–1160, Aug. 1994.

[15] M. Abramowitz and I. A. Segun, *Handbook of Mathematical Functions*. New York: Dover, 1972.

[16] Papoulis, *Random Variables, and Stochastic Processes, Probability*, 2nd ed. New York: McGraw-Hill, 1984.

Christophe Bourlier was born in La Flèche, France, on July 6, 1971. He received the "Electronic" DEA degree from the University of Rennes, France, in 1995 and the Ph.D. degree from the Electronic Systems and Computer Engineering Laboratory, Institut de Recherche et d'Enseignement Supèrieur aux Techniques de l'Electronique, University of Nantes, France, in 1999.

While at the University of Rennes, he was with the Laboratory of Radiocommunication, where he worked on antennas coupling in the VHF–HF band. He is now with Ecole Polytechnique de l'Université de Nantes, IRESTE, in the Systèmes Electroniques Télécom et RAdar group, which is associated with the Institut de Recherche en Communications et Cybernétique de Nantes, UMR no. 6597 CNRS. He works on the problems of electromagnetic scattering from rough surfaces in microwave and infrared bands.

Gérard Berginc was born in Etain, France, on March 25, 1959. He received the Dipl. Ing. degree from Ecole Nationale Supérieure de Physique, France, and the DEA degree in theoretical physics (with honors) from the University of Aix-Marseille, France, in 1983.

He was with Thomson-CSF, France, from 1985 to 1987 as a Research Engineer, where he was involved in development of radar performance calculation methods. From 1987 to 1990, he was with Mothesim, France, as Head of the Underwater Acoustic Research Department and as a Consultant for modeling in electromagnetic phenomena radar and space systems. From 1990 to 1991, he was with Thomson-CSF DAS as a Technical Expert in electromagnetic calculation methods. In 1991, he joined Thomson CSF Optronique, where he is currently Leader of a research group in the R&D department. His research activities include diffraction theory, high-frequency asymptotics, rough surface and random media scattering, localization effects, and frequency-selective surfaces. He is an URSI correspondent (Commissions B and F). He is the author of more than 80 journal articles, conference papers, and book chapters. He has received 20 patents.

Dr. Berginc is a member of the Electromagnetics Academy, SPIE.

Joseph Saillard was born in Rennes, France, in 1949. He received the Ph.D. and Docteur d'Etat degrees in physics from the University of Rennes, France, in 1978 and 1984, respectively.

From 1973 to 1988, he was with the University of Rennes as an Assistant Professor. He worked for CELAR Ministry of Defense (1985–1987) on radar signal processing. He is now a Professor with Ecole Polytechnique de l'Université de Nantes, France, at the Institut de Recherche et d'Enseignement Supèrieur aux Techniques de l'Electronique. He is in charge of the radar research team in the Systèmes Electroniques Télécom et RAdar, group which is associated with the Institut de Recherche en Communications et Cybernétique de Nantes, UMR no. 6597 CNRS. His fields of interest are radar polarimetry, adaptive antennas, and electronic systems. These activities are done in close collaboration with other public research organizations and industry. He is the organizer of JIPR '90, '92, '95, and '98.

Prof. Saillard is a member of the Electromagnetic Academy.